Subcritical Delamination of Dielectric and Metal Films from Low-k Organosilicate Glass (OSG) Thin Films in Buffered pH Solutions

Y. Lin[1], J.J. Vlassak[1], T.Y. Tsui[2], and A.J. McKerrow[2]
[1]DEAS, Harvard University, 29 Oxford Street, Cambridge, MA 02138, USA
[2]Silicon Technology Development, Texas Instruments Inc., Dallas, TX 75243, USA

ABSTRACT

Understanding subcritical fracture of low-k dielectric materials and barrier thin films in buffered solutions of different pH value is of both technical and scientific importance. Subcritical delamination of dielectric and metal barrier films from low-k organosilicate glass (OSG) films in pH buffer solutions was studied in this work. Crack path and subcritical fracture behavior of OSG depends on the choice of barrier layers. For the OSG/TaN system, fracture takes place in the OSG layer near the interface, while in OSG/SiN_x system, delamination occurs at the interface. Delamination behavior of both systems is well described by a hyperbolic sine model that had been developed previously based on a chemical reaction controlled fracture process at the crack tip. The threshold toughness of both systems decreases linearly with increasing pH value. The slopes of the reaction-controlled regime of the crack velocity curves for both systems are independent of pH as predicted by the model. Near transport-controlled regime behavior was observed in OSG/TaN system.

INTRODUCTION

Organosilicate glass (OSG) is one of the leading low-k dielectric materials for use as an interlayer dielectric (ILD) in high-performance interconnects. Due to the incorporation of organic groups (e.g., -CH3), the structure and surface chemical state of the OSG films are very different from those of conventional SiO_2. One of the main issues that arise when integrating low-k dielectric materials into a standard microfabrication process is the relatively poor adhesion between low-k dielectric materials and barrier layers. When subjected to stress in a chemically reactive environment, such as during chemical-mechanical polishing (CMP) or dicing, stress corrosion cracking can cause delamination of the barrier films. Although subcritical cracking of bulk silicate glass has been investigated [1], it is not well understood how the chemical agents in the environment affect subcritical fracture of barrier/low-k thin films structures. Here we report, for the first time, experimental results on subcritical cracking of OSG/TaN and OSG/SiN_x films in buffered pH solutions. These data were fitted and analyzed with a Sinh model developed previously [2-4].

EXPERIMENTAL

Subcritical delamination tests were conducted by means of the four-point bending technique. The detailed sample preparation technique and test procedures are described elsewhere [3]. Briefly, 500 nm OSG films with a dielectric constant of ~ 2.8 were grown on silicon wafers using a PECVD process. Subsequently, 80 nm SiN_x barrier films were deposited on top of the OSG films followed by a sputtered 40 nm Ti/400 nm Cu shielding layer. TaN/OSG films were

made by sputtering 30 nm TaN and 150 nm Cu on OSG. In order to make specimens, wafers with the film stack of interest were bonded to a supportive wafer using a spin-on epoxy. Finally, the bonded wafers were diced into 6 mm by 60 mm specimens and a notch was machined to within ~ 30 μm from the interface. The film stacks studied in this work are shown schematically in Figure 1.

Si	Si
80 nm SiN_x	80 nm SiN_x
5 μm epoxy	5 μm epoxy
40/400 nm Ti/Cu	150 nm Cu
80 nm SiN_x	30 nm TaN
500 nm OSG	500 nm OSG
Si	Si

Figure 1. Thin film stacks investigated OSG/barrier delamination in pH buffers

Samples were then tested on a four-point bend mechanical test system integrated with an environmental cell containing buffered acidic and basic solutions. Buffered pH solutions with pH values ranged from 3 to 12 were made using KOH, KCl and HCl solutions. The KCl solution was added to maintain a constant ionic strength (~ 0.122 M of Cl^-). Desired pH value was achieved by a titration process. The pH electrode was a FUTURA™ combined from BECKMAN. Before each measurement, the electrode was calibrated using standard pH buffer solutions from VWR. All samples were tested at ~ 26 C°.

The subcritical fracture tests included a preloading and a load-relaxation step. During preloading, the sample was loaded at a constant displacement rate until interfacial cracks were achieved. The load-relaxation process involved loading the sample to a certain load and fixing the displacement.

The energy release rate G (J/m^2) at the crack tip can be expressed as [5, 6]

$$G = \frac{21P^2l^2(1-\nu^2)}{16Eb^2h^3}, \quad (1)$$

where E and ν are the elastic modulus and Poisson's ratio of the Si substrate, P is the load, l is the distance between the inner and outer loading pins, b is the width of the specimen, and h is the wafer thickness. Noting that the compliance of the sample decreases when the crack grows along the interface, the crack velocity da/dt (m/s) can be calculated from beam theory [7]

$$v = \frac{1}{2}\cdot\frac{d(a_1+a_2)}{dt} = \frac{4Ebh^3}{21(1-\nu^2)l^2}\frac{d}{dt}\left(\frac{H}{P}\right), \quad (2)$$

where a_1 and a_2 denote the crack length of the two cracks, and H is the deflection of the beam.

After testing, the cracked samples were carefully opened and examined using X-ray photoelectron spectroscopy (XPS) to determine the crack path. A high-resolution atomic force microscope (AFM) was used to check the morphology of the crack surface at the crack tip.

RESULTS AND DISCUSSION

Figure 2 (a) shows that the crack path lies along the SiN_x/OSG interface for SiN_x/OSG samples. Our previous subcritical delamination study [3] showed that for the TaN/OSG system in an ambient environment with controlled relative humidity, the crack path lies within the OSG layer at a distance of approximately 5 nm from the TaN/OSG interface. The thickness of the OSG remaining on the TaN surface was estimated using XPS depth profiling. In Figure 2 (b), Ta, N, Si, O and C signals are detected on the TaN surface without ion sputtering. Since the escape depth of photoelectrons is ~ 2 nm, this indicates that the thickness of the OSG layer remaining on the TaN surface is less than 2 nm. The difference with the results for the ambient environment may be attributed to dissolution of OSG in the pH buffer solution during the subcritical delamination test.

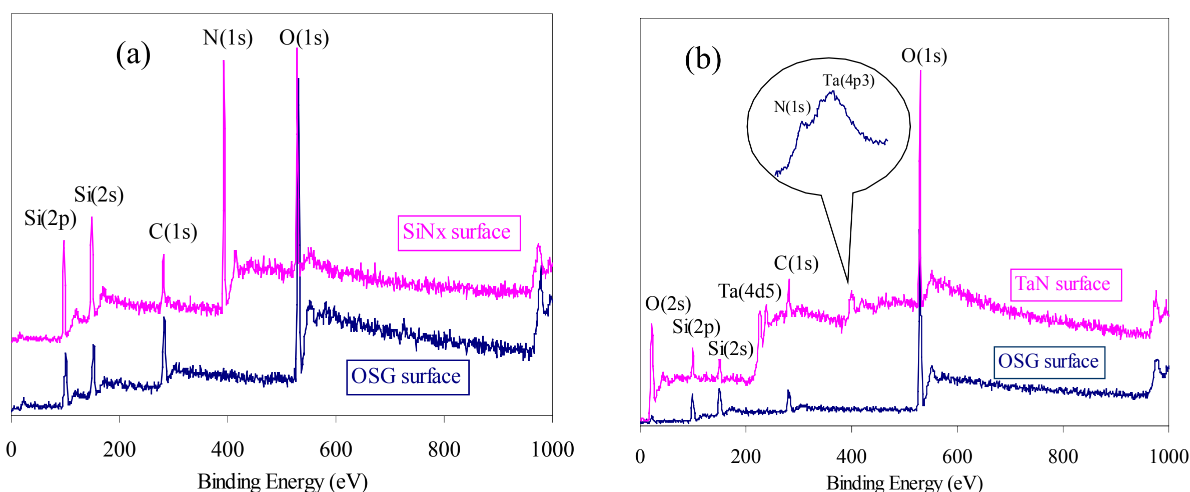

Figure 2. XPS spectra of cracking surfaces, (a) SiN_x/OSG, (b) TaN/OSG.

The AFM image shown in Figure 3 indicates that the roughness of the crack surface for the TaN/OSG system is several nanometers. This opens up the possibility that the TaN film is exposed in areas where the OSG has been completely dissolved. Morphologically, the feature size on the crack surface is in the range of 40 nm. This may be attributed to the heterogeneous nature of the microstructure of OSG considering the presence of methyl groups, voids and minor SiC phases [8], and the resulting non-uniform dissolution of the OSG film, which leads to the separation of the OSG by clusters of atoms.

Representative subcritical crack growth curves for both the OSG/TaN and OSG/SiN_x system are shown in Figure 4. These curves show that the pH value significantly affects the crack growth rate in the films. For a given energy release rate, the crack velocity in a basic solution can be several orders of magnitude higher than in an acidic solution. Increasing the pH also decreases the threshold energy release rate for both systems.

A lowered threshold energy release rate means that the crack will keep propagating at a lower driving force. Thus in a high-pH environment, a lower driving force is required for crack propagation to occur. Conversely, due to the accelerating effect of the high pH solution, it takes much less time for the crack to grow to significant size. These two factors are crucial to understanding the behavior of OSG/barrier systems in aqueous conditions. High pH solutions will not only make crack initiation easier, but will also accelerate crack growth significantly.

This can severely reduce the lifetime of OSG films if exposed to a CMP process where high pH slurries are used.

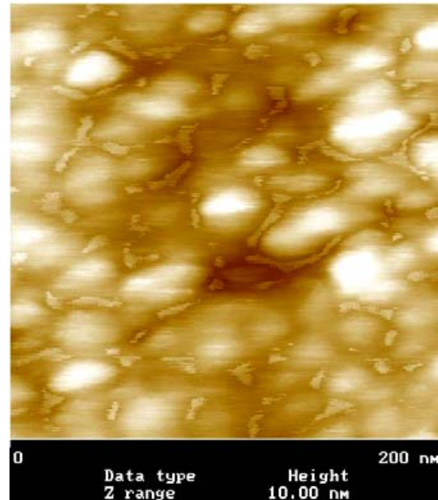

Figure 3. Morphology of fracture surface near the crack tip of a TaN/OSG sample.

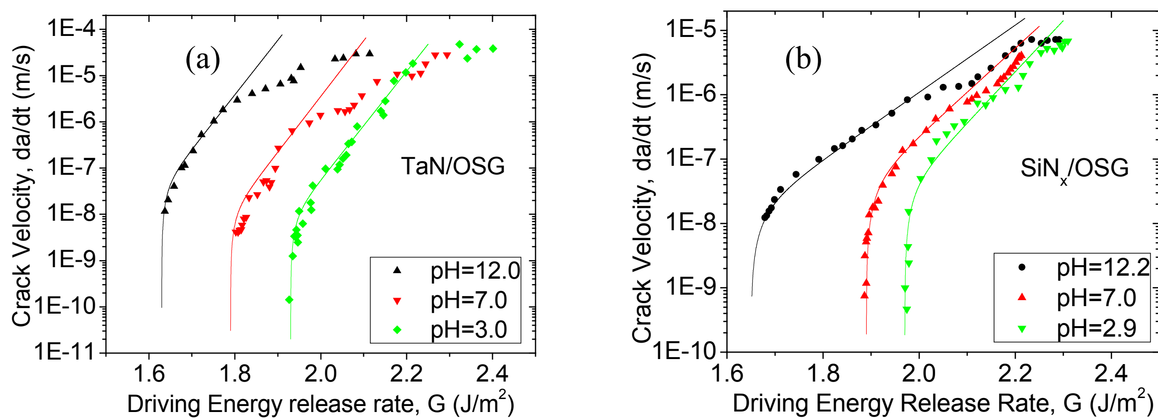

Figure 4. Subcritical crack growth curves showing the effect of solution pH value on crack velocity. (a) TaN/OSG; (b) SiN_x/OSG.

Figure 4 also shows that subcritical fracture behavior varies for different barrier layers, in addition to the selection of the crack path. Figure 4 (a) shows that the upper end of crack velocity in TaN/OSG is higher than in SiN_x/OSG system. At higher energy release rates, the crack velocity levels off indicating that fracture occurs in the transport-controlled regime for TaN/OSG films, especially for high pH curves. For SiN_x/OSG, on the other hand, such a region is not yet evident in these curves. This may be attributed to the different crack path followed in the two systems: for the SiN_x/OSG system, the crack lies along the SiN_x/OSG interface, while in the TaN/OSG system, it lies in the OSG layer. The crack surface for the TaN/OSG system is quite rough as shown in Figure 3, slowing down diffusion at the crack tip in the TaN/OSG system. Therefore, the subcritical fracture approaches the transport-controlled regime sooner in TaN/OSG than in SiN_x/OSG, when increasing the energy release rate.

The slope of the curves for TaN/OSG, as shown in Figure 4 with Sinh fitting, is found to be essentially independent of pH value. The crack velocity curves diverge from Sinh curves when the energy release rate increases, when mass transport at the crack tip is starting to limit the growth of the crack.

The mechanism of subcritical fracture behavior in pH solutions was analyzed quantitatively using a Sinh model based on a chemical reaction controlled fracture process and hydroxyl ion transport at the crack tip [2-4]. Considering the following reactions

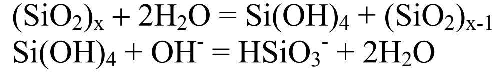

$$(SiO_2)_x + 2H_2O = Si(OH)_4 + (SiO_2)_{x-1}$$
$$Si(OH)_4 + OH^- = HSiO_3^- + 2H_2O$$

The crack velocity is described with the following equation

$$v = \frac{C_0 10^{-pOH}}{1 + C_1 \sinh\left(\dfrac{G-2\gamma}{2NkT}\right)} \sinh\left(\frac{G-2\gamma}{2NkT}\right), \qquad (3)$$

where C_0 is a constant associated to the materials structure and the chemical reaction at the crack tip, C_1 is related to the diffusion and chemical reaction, N is the number of bonds per unit area. 2γ is the threshold energy release rate, which is determined by

$$2\gamma = N\left(\Delta\mu^* - nkT\ln\left(10^{-pOH}\right)\right) = N\left(\Delta\mu^* + nkT\ln 10 \cdot pOH\right), \qquad (4)$$

where n is the order of reaction, and $\Delta\mu^*$ is the chemical potential changes of the reactions at the crack tip.

Fitting Equation (3) to the delamination rate data results in a bond density of $\sim 1.2 \times 10^{19}$ m^{-2}. This result is similar to that for previously investigated on SiO_2/OSG system as well as for bulk silicate glass [9]. The threshold energy release rates are shown in Figure 5. A linear dependence on pH value is observed in both systems as predicted by the model. The actual slope shown in Figure 5 is comparable to the slope predicted by Equation (4) within a factor of ~ 2.4 if first order kinetics is assumed.

The subcritical crack velocity curves predicted by the model are shown in Figure 6. When comparing to the curves in Figure 4, the model gives a good description of the subcritical fracture behavior of OSG/barrier systems near the threshold and in the reaction-controlled regime. The model also predicts that the crack velocity in the transport-controlled regime increases with increasing pH. However, this is not reflected in the experimental data. This would indicate that transport of the hydroxyl ions is not the rate limiting step, but possibly that of $HSiO_3^-$, which is much larger than the hydroxyl ion and will diffuse much more slowly.

CONCLUSIONS

Generally, the crack velocity in a basic solution is found to be orders of magnitude higher than in an acidic solution, while the crack path and subcritical fracture behavior of OSG in buffered pH solutions depend on the choice of barrier layers. The threshold energy release rate, G_{th}, of both OSG/TaN and OSG/SiN_x systems decreases linearly with increasing pH value. The slopes of the crack velocity curves in reaction-controlled regime of both systems are independent of pH. These behaviors are well described using a reaction-control-based model. It is also observed that the high end of the crack velocity curves of OSG/TaN system behave in a transport-controlled region, while it does not for the OSG/SiN_x system.

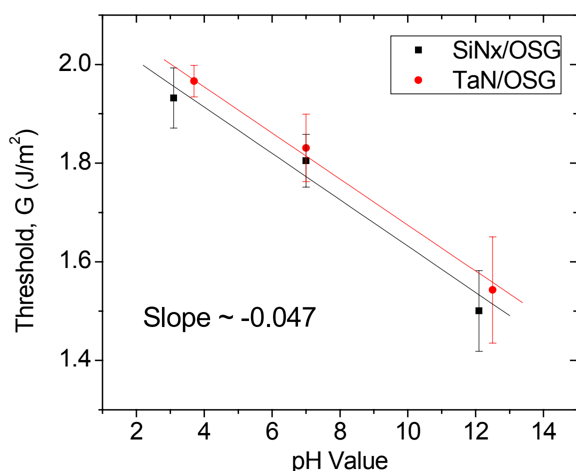

Figure 5. Threshold energy release rate decreases linearly with increasing pH value.

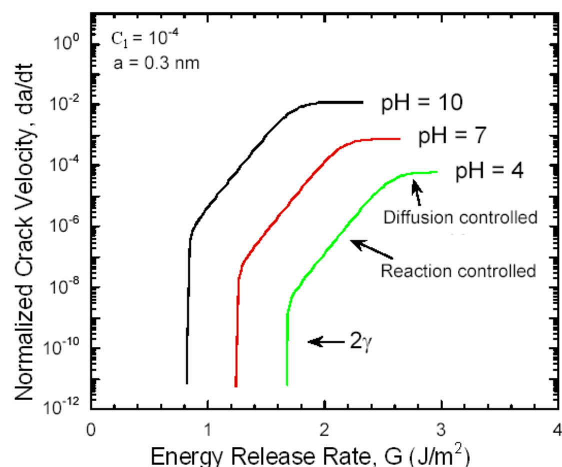

Figure 6. Subcritical crack velocity curves predicted by a Sinh model.

ACKNOWLEDGMENTS

Financial support from the Division of Engineering and Applied Sciences at Harvard University, from the Harvard MRSEC (DMR-98-09363), and from the National Science Foundation (DMR-0133559; DMR-0215902) are gratefully acknowledged.

REFERENCES

1. S. M. Wiederhorn and H. Johnson, *Journal of The American Ceramic Society,* **56** (4), 192 (1973).
2. R. E. Cook and E. G. Liniger, *Journal of The American Ceramic Society,* **76** (5), 1096 (1993).
3. Y. Lin, J. J. Vlassak, T.Y. Tsui and A.J. McKerrow, *MRS Proceedings,* **766**, E9.4 (2003).
4. M. W. Lane, J. M. Snodgrass and R. H. Dauskardt, Environmental effects on interfacial adhesion. *Microelectron. Reliability*, **41**, 1615–1624 (2001).
5. P. G. Charalambides, J. Lund, A. G. Evans and R. M. McMeeking, *Journal of Applied Mechanics,* **56**, 77 (1989).
6. Q. Ma, H. Fujimoto, P. Flinn, V. Jain, F. Adibi-Rizi, F. Moghadam and R. H. Dauskardt, in *Materials Reliability in Microelectronics V,* edited by A. S. Oates, W. F. Filter, R. Rosenberg, A. L. Greer and K. Gadepally (Mater. Res. Soc. Symp. Proc. **391**, Pittsburgh, PA, 1995), pp. 91-96.
7. Q. Ma, *Journal of Materials Research,* **12** (3), 840 (1997).
8. V. Ligatchev, T. K. S. Wong, B. Liu and Rusli, *Journal of Applied Physics,* **92** (8), 4605-4611 (2002).
9. S. M. Wiederhorn, *Journal of The American Ceramic Society,* **50** (8), 407 (1967).